Crossed magnetic fields technique for studying spin and orbital properties of 2d electrons in the dilute regime

M.E. Gershenson[a,*], V.M. Pudalov[a,b], H. Kojima[a], N. Butch[a], E.M. Dizhur[c], G. Brunthaler[d], A. Prinz[d], G. Bauer[d]

[a]Department of Physics and Astronomy, Rutgers University, NJ 08854, USA
[b]P.N. Lebedev Physics Institute, 117924 Moscow, Russia
[c]Institute for High Pressure Physics, Troitsk, Russia
[d]Institut für Halbleiterphysik, Johannes Kepler Universtät, Linz, Austria

Abstract

We developed a crossed magnetic field technique, which allowed us to probe separately the spin and orbital properties of two-dimensional (2D) electrons. Using this technique, we measured directly the spin susceptibility, the effective electron mass and g-factor in diluted 2D systems near the metal–insulator transition. All these quantities increase gradually with decreasing electron density: e.g., the susceptibility increases by a factor of 4 at $n \simeq 1 \times 10^{11}$ cm^{-2}. We have also studied the effect of the in-plane magnetic field $B_{||}$ on dephasing. At high electron densities ($n \geqslant 2.5 \times 10^{11}$ cm^{-2}), the dephasing time τ_φ decreases with $B_{||}$ much stronger than the momentum relaxation time τ. At small n, on the contrary, the increase of the dephasing rate with $B_{||}$ is less than that for τ. In the latter case, the dependence $\tau_\varphi(B_{||})$ can be attributed to enhancement of dephasing by the $B_{||}$-induced disorder. © 2002 Elsevier Science B.V. All rights reserved.

PACS: 71.30.+h; 73.20.Qt; 73.40.-c

Keywords: Metal–insulator transition; Two-dimensional electron gas; Magnetoresistance

1. Introduction

The physical properties of strongly correlated electron liquids are in the focus of experimental and theoretical studies. In particular, the two-dimensional (2D) metal–insulator transition (MIT), observed in diluted electron systems, might be driven by interactions (for reviews see, e.g., Refs. [1–3]). The strength of electron–electron interactions, which is characterized by the ratio r_s of the Coulomb interaction energy to the Fermi energy ε_F, increases with decreasing carrier density n. Very little is still known about parameters of electron liquids at such high values of $r_s \sim 10$, at which the 2D MIT is observed.

The theory of electron liquid predicts an r_s-dependent renormalization of the effective g^*-factor and the electron mass m^* [4]. Though the quantitative theoretical results [5–7] vary considerably, all of them suggest increases of m^* and g^* with r_s, and a ferromagnetic type of interactions at high r_s values ($r_s > 1$). Earlier experiments [8–11] have shown growth of m^* and g^* at $r_s \sim 1$–6. Potentially, strong interactions might drive the electron system towards ferromagnetic instability [4]. Moreover, it has been suggested that

* Corresponding author. Fax: +1-732-445-4343.
  E-mail address: gersh@physics.rutgers.edu
(M.E. Gershenson).

the 'metallic' behavior in 2D is accompanied by a tendency for a ferromagnetic instability [12].

Usually, information on m^* and g^* is provided by the Shubnikov–de Haas (SdH) measurements. To probe separately orbital and spin degrees of freedom, it is convenient to apply two independently varied magnetic field components: (a) $B_\perp$, normal to the 2D electron plane, which affects both orbital and spin degrees of freedom, and (b) the in-plane field $B_{||}$, which is coupled only to spins. Development of this novel experimental technique enabled us to explore the effect of $B_{||}$ on the electron spectrum and on the dephasing processes, as well as to measure directly m^* and g^* in strongly correlated systems near the 2D MIT.

2. Experimental technique

The conventional technique to measure the effective g-factor [8,10] is based on SdH measurements in magnetic fields tilted with respect to the 2DEG plane. In these measurements, the cyclotron energy, which is related to $B_\perp$, is compared with the Zeeman splitting, which depends on the total field, B_{tot}. To have a good control of both fields, the angle is to be measured with a very high accuracy, a difficult task at mK temperatures. We made the measurements more convenient by adding a second solenoid and taking data in crossed magnetic fields, which can be varied independently of each other (see Fig. 1). Application of $B_{||}$ facilitates the analysis of SdH oscillations, especially near the 2D MIT [13].

The resistivity measurements were performed at a low (13 Hz) frequency over the bath temperature range $T = 0.05$–1.6 K for three ($1\,0\,0$) Si-MOS samples selected from three wafers: Si12 (peak mobility 3.4 m^2/V s at $T = 0.3$ K), Si22 (3.2 m^2/V s), and Si6-14 (2.4 m^2/V s). The gate oxide thickness was 190 ± 20 nm for all the samples.

3. Measurements of χ^*, g^* and m^*

Typical traces of the longitudinal resistivity ρ_{xx} as a function of $B_\perp$ are shown in Fig. 2. Due to the high electron mobility, oscillations were detectable down to $B_\perp = 0.25$ T and the large number of oscillations (up to 120) enabled us to extract the fitting parameters
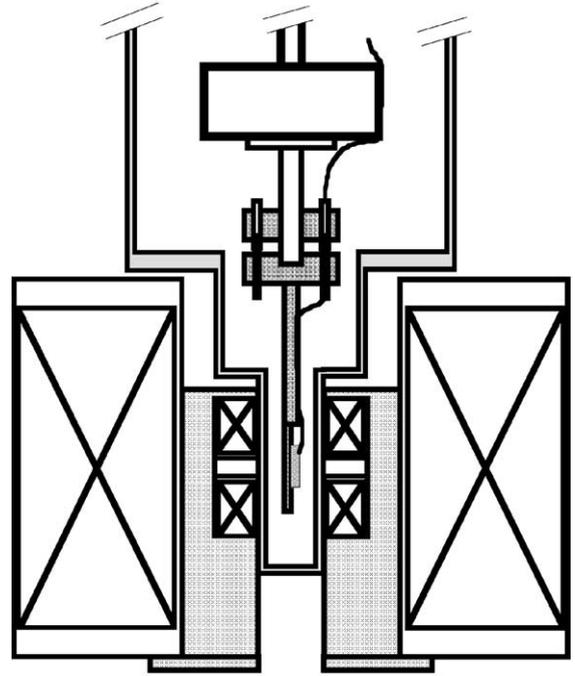

Fig. 1. The crossed magnetic field setup. The main superconducting solenoid provides the in-plane magnetic field $B_{||}$ up to 8 T. The superconducting split coils, positioned inside the main solenoid, produce the normal field $B_\perp$, which can be as large as 1.5 T at $B_{||} \leqslant 4$ T, and decreases gradually down to 0.6 T at $B_{||} = 7.5$ T. The sample (Si MOSFET) is attached to the cold finger of the mixing chamber, it is centered with respect to the split coils with its plane perpendicular to the axis of the coils.

g^* and m^* with a high accuracy. The oscillatory component $\delta\rho_{xx}$ was obtained by subtracting the monotonic "background" magnetoresistance from the measured $\rho_{xx}(B_\perp)$-dependence.

The oscillatory component of the magnetoresistance is given by theory [14] as follows:

$$\frac{\delta\rho_{xx}}{\rho_0} = \sum_s A_s \cos\left[\pi s\left(\frac{\hbar\pi n}{eB_\perp} - 1\right)\right] Z_s, \qquad (1)$$

where

$$A_s = 4\exp\left(-2\pi^2 s\frac{k_B T_D}{\hbar\omega_c}\right)\frac{2\pi^2 s k_B T/\hbar\omega_c}{\sinh(2\pi^2 s k_B T/\hbar\omega_c)}. \qquad (2)$$

Here, $\rho_0 = \rho_{xx}(B_\perp = 0)$, $\omega_c = eB_\perp/m^* m_e$ is the cyclotron frequency, m^* is the dimensionless effective mass, m_e is the free electron mass, and T_D is the Dingle temperature. We take the valley degeneracy $g_v = 2$ in Eqs. (1) and (2). The Zeeman term $Z_s = \cos[\pi s\hbar\pi$
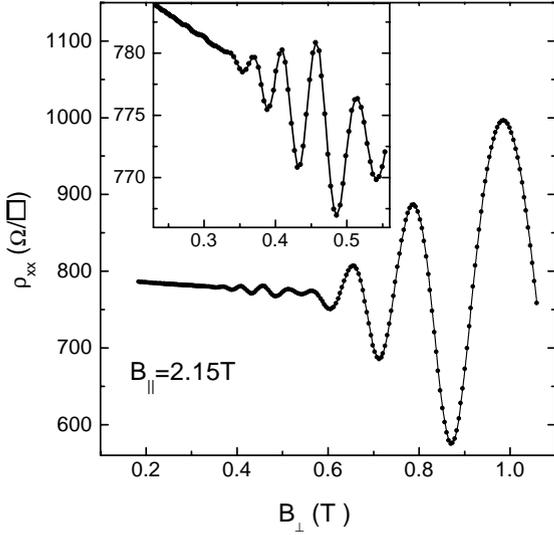
Fig. 2. Shubnikov–de Haas oscillations for sample Si6-14 ($n = 3.76 \times 10^{11}$ cm^{-2}) at $B_{||} = 2.15$ T and $T = 0.2$ K. The inset is the blow-up of the low-field region $B_\perp = 0.25 - 0.55$ T.

$(n_\uparrow - n_\downarrow)/(eB_\perp)]$ reduces to a field-independent constant for $B_{||} = 0$. Application of $B_{||}$ induces beating of SdH oscillations which are observed as a function of $B_\perp$. The beat frequency is proportional to the spin polarization of the interacting 2D electron system:

$$P = \frac{n_\uparrow - n_\downarrow}{n} = \frac{\chi^* B_{\text{tot}}}{g_b \mu_B n} = g^* m^* \frac{B_{\text{tot}}}{v B_\perp}, \qquad (3)$$

where $n_\uparrow$ ($n_\downarrow$) stands for the density of spin-up (spin-down) electrons, $\chi^* \propto g^* m^*$ is the Pauli spin susceptibility [15], $g_b \simeq 2$ is the bare g-factor for Si, $B_{\text{tot}} = \sqrt{B_\perp^2 + B_{||}^2}$, and $v = nh/eB_\perp$ is the filling factor of the Landau levels.

We have by now observed numerous SdH oscillations under a variety of conditions of electron density, field and temperature. The positions of the nodes give us $g^* m^*$ with a high accuracy. The phase of SdH oscillations change by π through the nodes as required by the variation of Z_s in Eqs. (1)(see Fig. 3). The positions of the nodes (i.e., the value of $g^* m^*$) are independent (within $\sim 2\%$ accuracy) of temperature for $T < 1$ K. We have observed a non-monotonic dependence of $g^* m^*$ on $B_{||}$: it is more pronounced near the 2D MIT, where $g^* m^*$ varies with $B_{||}$ by $\sim 15\%$. The data discussed below were obtained in the limit $B_{||} \to 0$.

(a)

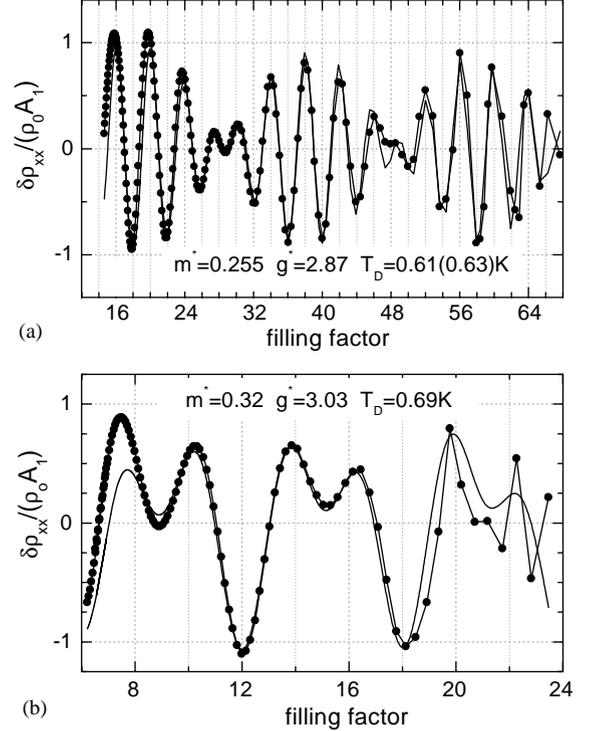(b)

Fig. 3. Examples of data fitting for sample 6-14 with Eq. (1): (a) $n = 3.76 \times 10^{11}$ cm^{-2}, $T = 0.2$ K, $B_{||} = 2.15$ T, $P = 20\%$; and (b) $n = 1.815 \times 10^{11}$ cm^{-2}, $T = 0.2$ K, $B_{||} = 2.5$ T, $P = 64\%$. The data are shown as dots, the fits (with parameters shown) as the thick solid lines. Both are normalized by $A_1(B_\perp)$: the normalization assigns equal weights to all oscillations. In Fig. 2a, the Dingle temperatures differ for spin-up and spin-down sub-bands.

Our data normalized to the first harmonic are shown as dots in Fig. 3 for two carrier densities. Fits with parameters as given are shown by the solid lines. The oscillations are plotted as a function of the filling factor $v = nh/eB_\perp$. We analyzed SdH oscillations over the low-field range $B_\perp \leqslant 1$ T to satisfy the assumption in Eq. (1) that $\hbar \omega_c \ll \varepsilon_F$ and $\delta \rho_{xx}/\rho_0 \ll 1$. Under the assumption, the inter-level interaction can be neglected.[1] The assumption might be violated for $v \leqslant 9$.

---

[1] The oscillatory behavior of the g^*-factor in strong $B_\perp$ is related to the exchange interaction between Landau levels (see, e.g., Ref. [4]). Particularly, this interaction leads to the enhancement of the g^*-value averaged over the period of oscillations (for the Si data, see Ref. [16]). For low magnetic fields and weak SdH effect regime, the inter-level interaction may be ignored.

Fitting procedure gives us g^*m^* and $(T + T_D)m^*$. Our data should be compared with the earlier data by Fang and Stiles [8] and Okamoto et al. [10]. The interesting question of criticality at or near MIT will require careful consideration. A possible spontaneous polarization by the electrons may be searched for by measuring changes in oscillation period at low fields. This search is also in progress.

It can be seen from Eq. (2) that the amplitude of oscillation is mainly controlled by $(T + T_D)m^*$. Preliminary analysis of the temperature dependence of the amplitude shows that T_D does not depend much on temperature.[2] If T_D can be taken to be independent of temperature, we obtain m^* as shown in Fig. 4b. This condition of T_D is almost certain to be violated near MIT. To reduce the uncertainty of m^* at large r_s, it is necessary to separate the effects of T-dependent scattering and 'smearing' of the Fermi distribution in the dependence $R(T)$; the adequate theory is currently unavailable. Our $m^*(r_s)$ data extend the range of electron densities explored earlier by Smith and Stiles [9] and by Pan et al. [11]. The g-factor values shown in Fig. 4c were obtained by dividing the g^*m^* data by the smooth approximation of the experimental dependence $m^*(r_s)$ shown in Fig. 4b.

4. Measurements of τ_φ

Measurements of τ_φ on the "metallic" side of the 2D MIT provide an important novel information about scattering processes and might shed light on the nature of still puzzling strong magnetoresistance induced by $B_{||}$. To estimate τ_φ, we measured the weak-localization (WL) magnetoresistance over the range $B_\perp = 0$–0.1 T for different values of $B_{||} = 0$–8 T. The measurements have been performed over the temperature range $T = 0.2$–1.1 K for the carrier concentrations $n = (1.2 - 11) \times 10^{11}$ cm^{-2}. For all the values of $B_{||}$, the WL MR can be fitted very well with the conventional WL theory (see, e.g., Ref. [17]), even in the vicinity of the 2D MIT (see Fig. 5).

---

[2] Below 0.3 K, we observed simultaneous trend of saturation in the temperature dependences of ρ_0, $\delta\rho_{xx}$, and the dephasing rate, which is presumably caused by electron overheating due to external electromagnetic noise.
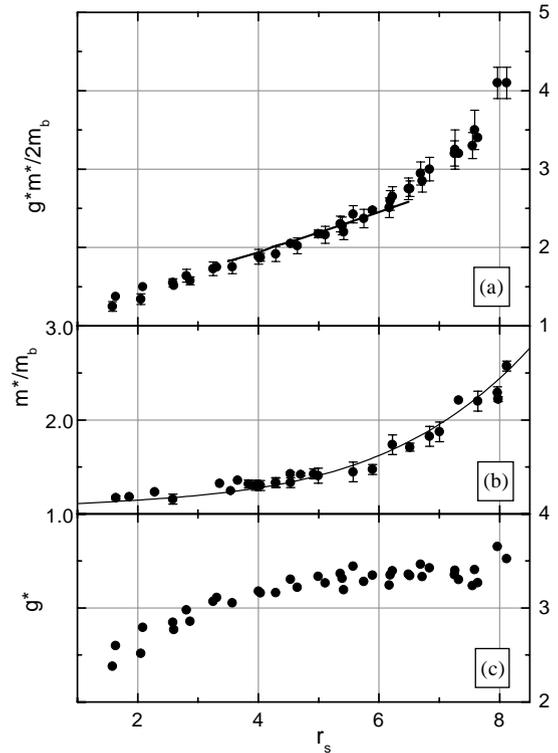

Fig. 4. Parameters g^*m^*, m^*, and g^* for different samples as a function of r_s (dots). At the MIT, the critical r_s-value for different samples ranges from $r_c = 7.9$ to 8.8; in particular, $r_c = 8.3$ for sample Si6-14 which has been studied down to the MIT. Solid dots in (b,c) show m^* and g^* calculated on the assumption that the Dingle temperature is T-independent. The solid line on panel (a) shows the data by Okamoto et al. [10].

At $T \geqslant 0.2$–0.3 K, the experimental dependences $\tau_\varphi^{-1}(T)$ can be described as the sum of two contributions: (a) the 2D Landau damping $1/\tau_{\varphi 0} \propto T^2 \ln(T)$ (see, e.g., Ref. [18]), and (b) the 2d quasi-elastic electron–electron scattering $1/\tau_\varphi^N \propto T$ (the so-called Nyquist dephasing) [19]. The second contribution, described by the following theoretical expression [19]:

$$\tau_\varphi^{-1} = \frac{\pi k_B T}{\hbar} \frac{e^2 R_\square}{2\pi^2 \hbar} \ln \frac{\pi \hbar}{e^2 R_\square} \qquad (4)$$

dominates at lower temperatures. Usually, this expression underestimates the experimental values of τ_φ^{-1} by a factor of 2–4 [19,20].

With increasing $B_{||}$, τ_φ decreases for all carrier concentrations (see Figs. 6 and 7). Though this ef-
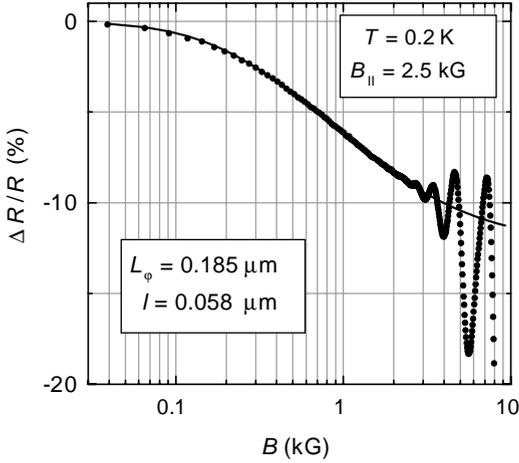
Fig. 5. The magnetoresistance of the 2DEG with $n = 1.32 \times 10^{11}$ cm^{-2} and $\rho_{xx} = 4.3$kΩ/□. The solid line is the WL fit with the following parameters: the dephasing length $L_\varphi = 0.185$ μm and the electron mean free path $l = 0.058$ μm. The range of $B_\perp$, where the WL theory is applicable, is limited only by the onset of SdH oscillations, and the agreement is very impressive even for low n, where the sheet resistance ρ_{xx} is as large as a few kΩ/□.

Fig. 6. The dependence of τ_φ on the sheet resistance $\rho_{xx} \equiv R_\square$, measured at $T = 0.3$ K for $n = 2.1 \times 10^{11}$ cm^{-2} (the increase of ρ_{xx} is induced by the in-plane magnetic field). Initial increase of τ_φ in small fields reflects the fact that the diffusion constant decreases with $B_{||}$ faster than L_φ: the dependence $L_\varphi(B_{||})$ is monotonic for all $B_{||}$. The solid line is the theoretical prediction for the Nyquist dephasing (Eq. (3)), normalized by a factor of 4 (this factor ~ 2–4 is common for all two-dimensional systems, both metallic and semiconducting [19,20]).
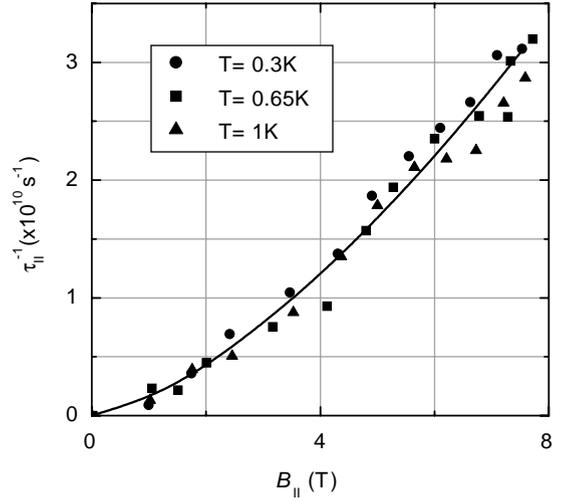

Fig. 7. The $B_{||}$-dependence of an additional field-induced dephasing rate $(\tau_{||})^{-1} = (\tau_\varphi)^{-1}(T, B_{||}) - (\tau_\varphi)^{-1}(T, B_{||} = 0)$, measured at $n = 10.6 \times 10^{11}$ cm^{-2} for different temperatures. The solid line is the dependence $(\tau_{||})^{-1} = 1.5 \times 10^9 B^{3/2}$.

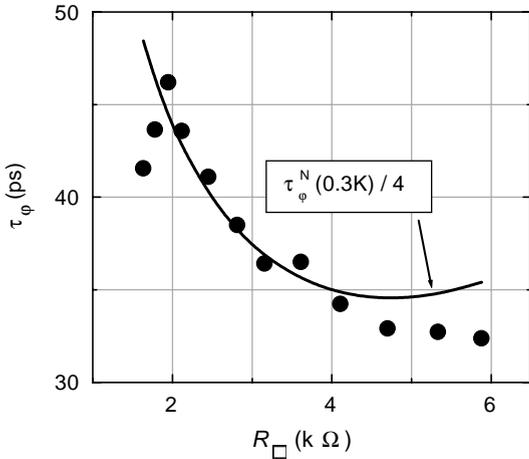fect is qualitatively similar over the whole range of $n = (1.2-11) \times 10^{11}$ cm^{-2}, drastically different dependences of the momentum relaxation time $\tau(B_{||})$ observed for low and high n, suggest that the underlying mechanism of the $\tau_\varphi(B_{||})$ decrease might be different in these two cases.

At high carrier densities ($n > 4 \times 10^{11}$ cm^{-2}), the decrease of τ_φ with $B_{||}$ is much more pronounced than the decrease of the momentum relaxation time τ (the in-plane magnetoresistance is relatively small at $B_{||} \leqslant 8$ T). Thus, the observed drop of τ_φ cannot be accounted by enhancement of the Nyquist dephasing, which is sensitive to disorder (see Eq. (4)). Several mechanisms can result in decrease of τ_φ with $B_{||}$ in this regime. Firstly, Mensz and Wheeler [21] proposed that, because of the Si–SiO$_2$ interface roughness, $B_{||}$ couples to the orbital motion of 2d electrons (the roughness 'transforms' a uniform $B_{||}$ into a random $B_\perp$), an electron picks up a random Berry's phase [22], and this enhances dephasing. Secondly, Falko [23] pointed out that $B_{||}$ couples different sub-bands of size quantization. In the presence of asymmetric scatterers with respect to the middle of a quantum well, this should result in the $B_{||}$-enhanced dephasing even for an ideally flat interface [23,24].

Finally, there might be other scenarios, for instance, an enhancement of spin–flip scattering due to a $B_{||}$-driven increase of the density of localized spins.

In the case of low $n \sim (1.2–2.5) \times 10^{11}$ cm^{-2}, $B_{||}$ induces a very strong positive magnetoresistance [25]: e.g., at $n = 2.1 \times 10^{11}$ cm^{-2}, the sheet resistance $R_\square$ increases by a factor of 3.6 when we apply $B_{||} = 7.6$ T (see Fig. 6). The Nyquist mechanism should result in decreasing τ_φ with increase of $R_\square$, and, indeed, Fig. 6 shows that at low temperatures, when the Nyquist dephasing dominates, the magnitude of the τ_φ decrease is in agreement with prediction of the theory [19]. Thus, at low n, the primary effect of $B_{||}$ on τ_φ can be ascribed to the $B_{||}$-enhanced disorder [25]. Note, that in the case of low n, the elastic scattering time τ is affected by $B_{||}$ stronger than τ_φ (see Fig. 6).

5. Conclusions

We developed the crossed magnetic field technique, and demonstrated that it is a powerful tool for studying 2D electron systems in the dilute limit. Using this technique, we measured Shubnikov–de Haas oscillations in independently controlled $B_\perp$ and $B_{||}$ over a broad range of carrier densities $n = (1 - 50) \times 10^{11}$ cm^{-2}. From these measurements, we determined the spin susceptibility $\chi^* \propto g^* m^*$, the effective mass m^* and g^*-factor. All these quantities increase gradually with decreasing electron density: at the lowest density $n = 1 \times 10^{11}$ cm^{-2} (i.e. $r_s = 8.3$), $g^* m^*$ is renormalized by a factor of ~ 4. It is an open question whether the moderate increase of χ^* is a precursor of spontaneous spin polarization [26]: our preliminary data do not support its occurrence at $n = n_c$, although this does not rule out such possibility at lower densities ($\leqslant 0.8 \times 10^{11}$ cm^{-2}). We have also observed the increase of the dephasing rate induced by the in-plane magnetic field. At small n, this increase can be attributed to the enhancement of dephasing by the $B_{||}$-induced disorder.

Acknowledgements

References

[1] E. Abrahams, S.V. Kravchenko, M.P. Sarachik, Rev. Mod. Phys. 73 (2001) 251.
[2] B.L. Altshuler, D.L. Maslov, V.M. Pudalov, Physica E 9 (2001) 209.
[3] B.L. Altshuler, G.W. Martin, D.L. Maslov, V.M. Pudalov, A. Prinz, G. Brunthaler, G. Bauer, cond-mat/0008005.
[4] A.A. Abrikosov, Fundamentals of the Theory of Metals, North-Holland, Amsterdam, 1988.
[5] A. Isihara, Electron Liquids, Springer, Berlin, 1997; N. Iwamoto, Phys. Rev. B 43 (1991) 2174.
[6] Y. Kwon, D.M. Ceperley, R.M. Martin, Phys. Rev. B 50 (1994) 1684.
[7] G.-H. Chen, M.E. Raikh, Phys. Rev. B 60 (1999) 4826.
[8] F.F. Fang, P.J. Stiles, Phys. Rev. B 174 (1968) 823.
[9] J.L. Smith, P.J. Stiles, Phys. Rev. Lett. 29 (1972) 102.
[10] T. Okamoto, K. Hosoya, S. Kawaji, A. Yagi, Phys. Rev. Lett. 82 (1999) 3875.
[11] W. Pan, D.C. Tsui, B.L. Draper, Phys. Rev. B 59 (1999) 10 208.
[12] A.M. Finkelstein, Sov. Sci. Rev. A 14 (1990) 3.
[13] V.M. Pudalov, M.E. Gershenson, H. Kojima, N. Butch, E.M. Dizhur, A. Prinz, G. Brunthaler, G. Bauer, cond-mat/0105081.
[14] I.M. Lifshitz, A.M. Kosevich, Zh. Eksb. Teor. Fiz. 29 (1955) 730; A. Isihara, L. Smrčka, J. Phys. C 19 (1986) 6777.
[15] E.M. Lifshitz, L.P. Pitaevskii, Statistical Physics, Part II, Pergamon Press, Oxford, 1980.
[16] V.M. Pudalov, et al., JETP 62 (1985) 1079.
[17] B.L. Altshuler, A.G. Aronov, M.E. Gershenson, Yu.V. Sharvin, Sov. Sci. Rev. A 9 (1987) 223.
[18] M. Reizer, J.W. Wilkins, Phys. Rev. B 55 (1997) R7363.
[19] B.L. Altshuler, A.G. Aronov, D.E. Khmelnitskii, J. Phys. C 15 (1982) 7367.
[20] G. Brunthaler, A. Prinz, G. Bauer, V.M. Pudalov, Phys. Rev. Lett. 87 (2001) 096802.
[21] P.M. Mensz, R.G. Wheeler, Phys. Rev. B 35 (1987) 2844.
[22] H. Mathur, H.U. Baranger, cond-mat/0008375.
[23] V.I. Falko, J.Phys.: Condens. Matter 2 (1990) 3797.
[24] J.S. Meyer, A. Altland, B.L. Altshuler, cond-mat/0105623.
[25] V.M. Pudalov, G. Brunthaler, A. Prinz, G. Bauer, cond-mat/0103087.
[26] A.A. Shashkin, S.V. Kravchenko, V.T. Dolgopolov, T.M. Klapwijk, Phys. Rev. Lett. 87 (2001) 086801; S.A. Vitkalov, M.P. Sarachik, T.M. Klapwijk, Phys. Rev. Lett. 87 (2001) 086401.